Available online at www.sciencedirect.com
SCIENCE DIRECT®
Inorganica Chimica Acta 359 (2006) 863–876
Inorganica Chimica Acta
www.elsevier.com/locate/ica

Synthesis and characterization of ruthenium and osmium complexes of heterocyclic bidentate ligands (N, X), X = S, Se

Antonio Sousa-Pedrares [a], Maria Luz Durán [a], Jaime Romero [a], José Arturo García-Vázquez [a], Juan C. Monteagudo [b], Antonio Sousa [a,*], Jonathan R. Dilworth [c]

[a] *Departamento de Química inorgánica, Universidad de Santiago de Compostela, 15782 Santiago de Compostela, Spain*
[b] *Departamento de Química Física, Universidad de Santiago de Compostela, 15782 Santiago de Compostela, Spain*
[c] *Inorganic Chemistry Laboratory, University of Oxford, Oxford OXI 3QR, UK*

Received 5 April 2005; accepted 11 June 2005
Available online 19 August 2005

Ruthenium and Osmium Chemistry Topical Issue.

Abstract

The reaction of $[RuCl_2(PPh_3)_3]$ and $[OsBr_2(PPh_3)_3]$ precursors with a series of heterocyclic bidentate (N, X) ligands, X = S, Se, gave complexes $[M(R\text{-}pyS)_2(PPh_3)_2]$, (R = H, 3-$CF_3$, 5-$CF_3$, 3-$Me_3Si$); $[M(R\text{-}pymS)_2(PPh_3)_2]$, (R = 4-$CF_3$, 4,6-$MeCF_3$) and $[M(R\text{-}pySe)_2(PPh_3)_2]$, (R = H, 3-$CF_3$, 5-$CF_3$), where M is Ru or Os, pyS and pymS the anions of pyridine-2-thione and pyrimidine-2-thione,respectively, and pySe is the anion produced by the reductive cleavage of the Se–Se bond in the dipyridyl-2,2′-diselenide. All of the compounds obtained were characterized by microanalysis, IR, FAB, NMR spectroscopy and by cyclic voltammetry. Compounds $[Ru(3\text{-}CF_3\text{-}pyS)_2(PPh_3)_2]\cdot 2(CH_2Cl_2)$ (**2**), $[Ru(3\text{-}Me_3Si\text{-}pyS)_2(PPh_3)_2]$ (**4**), $[Ru(4\text{-}CF_3\text{-}pymS)_2(PPh_3)_2]$ (**5**), $[Ru(3\text{-}CF_3\text{-}pySe)_2(PPh_3)_2]\cdot 2(CH_2Cl_2)$ (**8**), $[Os(3\text{-}CF_3\text{-}pyS)_2(PPh_3)_2]\cdot(CHCl_3)$ (**11**), $[Os(3\text{-}Me_3Si\text{-}pyS)_2(PPh_3)_2]$ (**13**), $[Os(3\text{-}CF_3\text{-}pySe)_2(PPh_3)_2]\cdot 2(CH_2Cl_2)$ (**17**), $[Os(5\text{-}CF_3\text{-}pySe)_2(PPh_3)_2]\cdot 2(H_2O)$ (**18**) and $[OsCl_2(4,6\text{-}MeCF_3\text{-}pymS)(PPh_3)_2]$ (**19**) were also characterized by X-ray diffraction. In all cases, the metal is in a distorted octahedral environment with the heterocyclic ligand acting as a bidentate (N, S) chelate system.

Keywords: Ruthenium complexes; Osmium complexes; Heterocyclic thiones; Selenolates

1. Introduction

Metal complexes with heterocyclic thiones, mainly pyridine-2-thionato and pyrimidine-2-thionato complexes, have been widely studied because of their relevance to biological systems and the versatility in their coordination forms (neutral monodentate [1], bridging through S [2], anionic S-monodentate [3], chelating [4] or bridging between two [5] or three [6] metal atoms), which gives rise to complexes with variable nuclearity and a wide range of structural geometries [7]. The chemistry of Ru(II), and to a lesser extent Os(II), with the pyridine-2-thione ligand is relatively well documented for complexes with a variety of coligands such as phosphines, carbonyls or others that complete the coordination sphere around the metal [8–17]. Furthermore, the crystal structure of $[Ru(pyS)_2(PPh_3)_2]$ has already been reported [8]. However, there is experimental evidence that the presence and location of a substituent in the heterocyclic ring are important factors in determining the type of

* Corresponding author. Tel.: +34 981 563 100x14950; fax: +34 981 597 525.
E-mail addresses: qijagv@usc.es (J.A. García-Vázquez), qiansoal@usc.es (A. Sousa).

0020-1693/$ - see front matter © 2005 Elsevier B.V. All rights reserved.
doi:10.1016/j.ica.2005.06.009

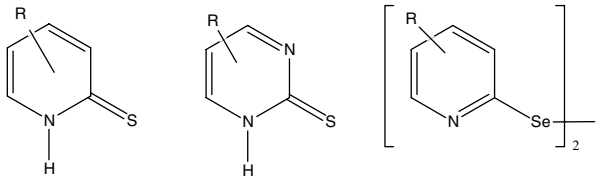

Scheme 1.

coordination of the ligand and the structure and properties of the metal–pyridine-2-thionato complexes [18–20]. On the other hand, complexes of these metals with pyrimidine-2-thione ligands has been studied to a much lesser extent [21–24] and compounds incorporating the pyridine-2-selenolato ligand have not been reported at all. Our continued interest in the coordination chemistry of heterocyclic thionato or selenolato ligands led us to investigate the synthesis and characterization of ruthenium and osmium compounds with a series of heterocyclic bidentate ligands (N,X), X = S, Se (see Scheme 1). The results of this study are reported here along with a discussion concerning the influence of the nature and the location of the substituent in the heterocyclic ring on the structure and properties of the complexes.

2. Experimental

2.1. General procedures

All manipulations were carried out under an inert atmosphere of dry nitrogen. $RuCl_3 \cdot 3H_2O$, OsO_4, PPh_3, 3-CF_3-pySH, 5-CF_3-pySH and other reagents were commercial products and were used without further purification. 3-Me_3Si-pySH was prepared following the method described by Block et al. [25]. 4,6-(Me,CF_3)-pymSH was synthesized by direct reaction of 1,1,1-trifluoro-2,4-pentanedione and thiourea as described in the literature [26]. The syntheses of $(pySe)_2$, (3-CF_3-$pySe)_2$ and (5-CF_3-$pySe)_2$ were carried out by reacting sodium diselenide with the appropriate 2-bromopyridine in dimethylformamide following a literature procedure [27]. $[RuCl_2(PPh_3)_2]$ was prepared using a procedure similar to that described by Hallman et al. [28] and $[OsBr_2(PPh_3)_3]$ was obtained using a procedure similar to that described by Hoffman and Caulton [29]. Elemental analyses were performed in a Carlo-Erba EA microanalyser. IR spectra were recorded on KBr discs using a Bruker IFS 66v spectrophotometer. ^1H and ^{13}C spectra were recorded on a Bruker AMX 300 MHz instrument using $CDCl_3$ as solvent. The chemical shifts for ^1H and ^{13}C were determined against TMS as internal standard. The FAB mass spectra were recorded on a Micromass Autospec instrument using 3-nitrobenzyl alcohol as the matrix material. Voltammograms were obtained with an apparatus consisting of an EG&G Priceton Applied Research potentiostat (model 273) and an electrochemical cell consisting of a working electrode (graphite disc), a reference electrode (saturated calomel) and an auxiliary electrode (platinum wire). Dichloromethane was used as the solvent to make the solutions and tetrabutylammonium tetrafluoroborate (0.1 M) was used as the electrolyte. In all cases, the concentration of the samples under investigation were 10^{-3} M.

2.2. Preparation of the complexes

2.2.1. $[Ru(pyS)_2(PPh_3)_2]$ (1)

Et_3N (0.1 ml, 0.688 mmol) was added to a methanolic solution of pySH (0.0696 g, 0.625 mmol). The resulting solution was stirred for 1 h and a solution of $[RuCl_2(PPh_3)_3]$ (0.3 g, 0.313 mmol) in dichloromethane was added. The reaction mixture was stirred for 2 h and the resulting solid was filtered off, washed with diethyl ether and dried under vacuum. *Anal.* Calc. for $C_{46}H_{38}N_2P_2S_2Ru$ (mol. wt. 845.9): C, 65.3; H, 4.5; N, 3.3. Found: C, 64.8; H, 4.7; N, 3.3%. IR (KBr): 3049 (m), 1578 (m), 1545 (m), 1480 (m), 1432 (s), 1419 (s), 1311 (w), 1262 (m), 1190 (w), 1151 (m), 1137 (m), 1097 (w), 1088 (m), 1028 (w), 752 (m), 740 (s), 696 (s), 539 (m), 521 (s), 500 (m), 470 (m). ^1H NMR ($CDCl_3$, ppm) 7.6 (H_6, d, 1H), 6.8 (H_3, d, 1H), 6.2 (H_4, t, 1H), 6.0 (H_5, t, 1H); 7.2–6.9 (m, 15H, PPh_3); ^{13}C NMR ($CDCl_3$, ppm) 181.2 (C_2), 124.2 (C_3), 136.1 (C_4): 115.3 (C_5), 146.0 (C_6), 128.2 (C_α), 133.8 (C_β), 126.7 (C_γ): 126.8 (C_δ). FAB (*m/z*): 846 (M^+), 736 (M–pyS), 584 (M–PPh_3) and 474 (M–pyS–PPh_3).

2.2.2. $[Ru(3\text{-}CF_3\text{-}pyS)_2(PPh_3)_2]$ (2)

3-CF_3-pySH (0.112 g, 0.625 mmol), Et_3N (0.1 ml, 0.688 mmol) and $[RuCl_2(PPh_3)_3]$ (0.3 g, 0.313 mmol). *Anal.* Calc. for $C_{48}H_{36}F_6N_2P_2S_2Ru$ (mol. wt. 981.9): C, 58.7; H, 3.7; N, 2.8. Found: C, 58.5; H, 3.6; N, 2.9%. IR (KBr): 3059 (m), 1578 (m), 1562 (m), 1481 (m), 1434 (m), 1404 (s), 1321 (s), 1259 (m), 1208 (m), 1165 (m), 1129 (m), 1110 (m), 1089 (m), 1066 (m), 1047 (m), 1001 (w), 972 (w), 813 (m), 797 (m), 740 (m), 721 (m), 696 (s), 535 (m), 521 (s), 497 (m). ^1H NMR ($CDCl_3$, ppm) 7.8 (H_6, d, 1H), 6.1 (H_5, t, 1H); 7.2–6.9 (m, 16H, H_4, PPh_3); ^{13}C NMR ($CDCl_3$, ppm) 181.0 (C_2), 131.1 (C_3), 135.5 (C_4): 113.9 (C_5), 149.0 (C_6), 128.5 (C_α), 133.9 (C_β), 127.0 (C_γ): 127.0 (C_δ). FAB (*m/z*): 982 (M^+), 804 (M–{3-CF_3-pyS}), 720 (M–PPh_3) and 542 (M–{3-CF_3-pyS}–PPh_3). Crystals of $[Ru(3\text{-}CF_3\text{-}pyS)_2(PPh_3)_2] \cdot 2(CH_2Cl_2)$ suitable for X-ray studies were obtained by crystallisation of the initial product from methanol/dichloromethane.

2.2.3. $[Ru(5\text{-}CF_3\text{-}pyS)_2(PPh_3)_2]$ (3)

5-CF_3-pySH (0.112 g, 0.625 mmol), Et_3N (0.1 ml, 0.688 mmol) and $[RuCl_2(PPh_3)_3]$ (0.3 g, 0.313 mmol).

Anal. Calc. for $C_{48}H_{36}F_6N_2P_2S_2Ru$ (mol. wt. 981.9): C, 58.7; H, 3.7; N, 2.8. Found: C, 59.1; H, 3.8; N, 2.8%. IR (KBr): 3052 (m), 1593 (s), 1548 (m), 1480 (m), 1460 (m), 1434 (m), 1383 (w), 1319 (s), 1269 (m), 1256 (m), 1170 (m), 1151 (s), 1116 (m), 1105 (m), 1072 (s), 1026 (w), 924 (w), 824 (m), 761 (m), 697 (s), 615 (w), 535 (m), 521 (s), 496 (m), 470 (m). ^{1}H NMR ($CDCl_3$, ppm) 7.68 (H_6, s, 1H), 7.1 (H_3, t, 1H), 6.3 (H_4, d, 1H); 7.2–6.9 (m, 15H, PPh_3); ^{13}C NMR ($CDCl_3$, ppm) 186.6 (C_2), 123.7 (C_3), 135.2 (C_4): 130.1 (C_5), 143.2 (C_6), 128.7 (C_α), 133.8 (C_β), 127.1 (C_γ): 127.1 (C_δ). FAB (*m*/*z*): 982 (M^+), 804 (M–{5-CF_3-pyS}), 720 (M–PPh_3) and 542 (M–{5-CF_3-pyS}–PPh_3).

2.2.4. [Ru(3-Me_3Si-pyS)$_2$(PPh_3)$_2$] (**4**)

3-TMS-pySH (0.115 g, 0.625 mmol), Et_3N (0.1 ml, 0.688 mmol) and [$RuCl_2(PPh_3)_3$] (0.3 g, 0.313 mmol). *Anal*. Calc. for $C_{52}H_{54}N_2P_2S_2Si_2Ru$ (mol. wt. 990.3): C, 63.0; H, 5.5; N, 2.8. Found: C, 63.0; H, 5.6; N, 2.7%. IR (KBr): 3048 (m), 1156 (m), 1541 (m), 1481 (m), 1432 (m), 1365 (s), 1261 (w), 1242 (m), 1221 (m), 1183 (w), 1135 (m), 1086 (m), 1072 (m), 1055 (m), 1027 (w), 840 (s), 746 (m), 695 (s), 625 (w), 536 (s), 523 (s), 498 (m), 468 (w). ^{1}H NMR ($CDCl_3$, ppm) 7.8 (H_6, d, 1H), 6.2 (H_4, t, 1H); 0.5 (CH_3, s, 9H); 7.2–6.9 (m, 16H, H_4, PPh_3); ^{13}C NMR ($CDCl_3$, ppm) 187.4 (C_2), 138.8 (C_3), 136.6 (C_4), 114.7 (C_5), 146.2 (C_6), 127.9 (C_α), 134.1 (C_β), 126.6 (C_γ): 126.7 (C_δ). FAB (*m*/*z*): 990 (M^+), 808 (M–{3-TMS-pyS}), 728 (M–PPh_3) and 546 (M–{3-TMS-pyS}–PPh_3). Crystals of [Ru(3-Me_3Si-pyS)$_2$(PPh_3)$_2$] suitable for X-ray studies were obtained by crystallisation of the initial product from methanol/dichloromethane.

2.2.5. [Ru(4-CF_3-pymS)$_2$(PPh_3)$_2$] (**5**)

4-CF_3-pymSH (0.1125 g, 0.625 mmol), Et_3N (0.1 ml, 0.688 mmol) and [$RuCl_2(PPh_3)_3$] (0.3 g, 0.313 mmol). *Anal*. Calc. for $C_{46}H_{34}F_6N_4P_2S_2Ru$ (mol. wt. 983.9): C, 56.1; H, 3.5; N, 5.7. Found: C, 56.3; H, 3.5; N, 5.6%. IR (KBr): 3450 (vb), 3047 (m), 1555 (m), 1481 (m), 1432 (m), 1347 (m), 1331 (s), 1265 (w), 1195 (s), 1163 (m), 1147 (m), 1113 (m), 1091 (m), 1026 (w), 1003 (m), 834 (m), 739 (m), 698 (s), 684 (m), 535 (s), 495 (m), 474 (w). ^{1}H NMR ($CDCl_3$, ppm) 7.7 (H_6, d, 1H), 6.3 (H_5, d, 1H); 7.2–6.9 (m, 15H, PPh_3); ^{13}C NMR ($CDCl_3$, ppm) 188.6 (C_2), 153.0 (C_4), 119.0 (C_5), 155.7 (C_6), 129.0 (C_α), 134.6 (C_β), 127.3 (C_γ): 127.4 (C_δ). FAB (*m*/*z*): 984 (M^+), 805 (M–{4-CF_3-pymS}), 722 (M–PPh_3) and 543 (M–{4-CF_3-pymS}–PPh_3). Crystals of [Ru(4-CF_3-pymS)$_2$(PPh_3)$_2$] suitable for X-ray studies were obtained by crystallisation of the initial product from methanol/dichloromethane.

2.2.6. [Ru(4,6-CF_3Me-pymS)$_2$(PPh_3)$_2$] (**6**)

4,6-CF_3Me-pymSH (0.1212 g, 0.625 mmol), Et_3N (0.1 ml, 0.688 mmol) and [$RuCl_2(PPh_3)_3$] (0.3 g, 0.313 mmol). *Anal*. Calc. for $C_{48}H_{38}F_6N_4P_2S_2Ru$ (mol. wt. 1012.1): C, 56.9; H, 3.8; N, 5.5. Found: C, 56.9; H, 4.0; N, 5.4%. IR (KBr): 3449 (vb), 3058 (m), 1578 (m), 1542 (s), 1482 (m), 1434 (s), 1395 (s), 1311 (w), 1274 (s), 1233 (m), 1197 (m), 1172 (m), 1147 (m), 1114 (m), 1089 (m), 1027 (w), 992 (m), 929 (m), 855 (m), 746 (m), 697 (s), 536 (m), 523 (s), 497 (m), 466 (w). ^{1}H NMR ($CDCl_3$, ppm) 6.13 (H5, s, 1H); 2.26 (CH_3, s, 3H) 7.2–6.9 (m, 15H, PPh_3); ^{13}C NMR ($CDCl_3$, ppm) 180.1 (C_2), 135.0 (C_4): 118.5 (C_5), 171.4 (C_6), 128.9 (C_α), 133.7 (C_β), 127.0 (C_γ): 127.1 (C_δ). FAB (*m*/*z*): 1012 (M^+), 819 (M–{4,6-CF_3Me-pymS}), 750 (M–PPh_3) and 557 (M–{4,6-CF_3Me-pymS}–PPh_3).

2.2.7. [Ru(pySe)$_2$(PPh_3)$_2$]·(CH_2Cl_2) (**7**)

A methanolic solution of dipyridyl-2,2′-diselenide (0.0983 g, 0.312 mmol) was treated with $NaBH_4$ (0.026 g, 0.688 mmol). The mixture was stirred for 1 h and a solution of [$RuCl_2(PPh_3)_3$] (0.3 g, 0.313 mmol) in dichloromethane was added. The reaction mixture was stirred for 3 h and the resulting solid filtered off under nitrogen, washed with diethyl ether and dried under vacuum (0.052 g, 30.4%). *Anal*. Calc. for $C_{47}H_{40}Cl_2N_2P_2Se_2Ru$ (dichloromethane solvate, mol. wt. 1024.7): C, 55.0; H, 3.9; N, 2.7. Found: C, 54.0; H, 4.2; N, 2.7%. IR (KBr): 3049 (m), 1579 (m), 1544 (m), 1480 (m), 1432 (m), 1416 (m), 1311 (w), 1260 (m), 1247 (w), 1148 (m), 1121 (m), 1096 (m), 1087 (m), 752 (m), 738 (s), 697 (s), 538 (m), 521 (s), 499 (m). ^{1}H NMR ($CDCl_3$, ppm) 8.0 (H_6, d, 1H), 6.7 (H_3, d, 1H), 6.4 (H_4, d, 1H), 6.1 (H_5, t, 1H); 7.2–6.9 (m, 15H, PPh_3); ^{13}C NMR ($CDCl_3$, ppm) 173.2 (C_2), 136.9 (C_4): 117.0 (C_5), 148.7 (C_6), 128.1 (C_α), 134.2 (C_β), 126.7 (C_γ): 126.8 (C_δ). FAB (*m*/*z*): 940 (M^+), 784 (M–pySe), 678 (M–PPh_3) and 522 (M–{pySe}–PPh_3).

2.2.8. [Ru(3-CF_3-pySe)$_2$(PPh_3)$_2$] (**8**)

(3-CF_3-pySe)$_2$ (0.141 g, 0.312 mmol), $NaBH_4$ (0.026 g, 0.688 mmol) and [$RuCl_2(PPh_3)_3$] (0.3 g, 0.313 mmol). *Anal*. Calc. for $C_{48}H_{36}F_6N_2P_2Se_2Ru$ (mol. wt. 1077.97): C, 53.4; H, 3.4; N, 2.6. Found: C, 53.2; H, 3.4; N, 2.6%. IR (KBr): 3051 (m), 1561 (m), 1542 (w), 1481 (m), 1433 (s), 1402 (s), 1319 (s), 1267 (w), 1247 (w), 1163 (m), 1128 (m), 1087 (m), 1058 (m), 1045 (m), 799 (m), 741 (s), 695 (s), 537 (m), 521 (s), 494 (m). ^{1}H NMR ($CDCl_3$, ppm) 8.4 (H_6, d, 1H), 7.4 (H_4, d, 1H), 6.5 (H_5, t, 1H), 7.3–7.1 (m, 15H, PPh_3). FAB (*m*/*z*): 1076 (M^+), 852 (M–{3-CF_3-pySe}), 814 (M–PPh_3) and 589 (M–{3-CF_3-pySe}–PPh_3). Crystals of [Ru(3-CF_3-pySe)$_2$(PPh_3)$_2$]·2(CH_2Cl_2) suitable for X-ray studies were obtained by crystallisation of the initial product from methanol/dichloromethane.

2.2.9. [Ru(5-CF_3-pySe)$_2$(PPh_3)$_2$] (**9**)

(5-CF_3-pySe)$_2$ (0.141 g, 0.312 mmol), $NaBH_4$ (0.026 g, 0.688 mmol) and [$RuCl_2(PPh_3)_3$] (0.3 g, 0.313 mmol).

Anal. Calc. for $C_{48}H_{36}F_6N_2P_2Se_2Ru$ (mol. wt. 1077.97): C, 53.4; H, 3.4; N, 2.6. Found: C, 53.1; H, 3.5; N, 2.7%. IR (KBr): 3450 (b), 3053 (m), 1597 (m), 1549 (w), 1480 (m), 1459 (w), 1434 (m), 1377 (w), 1323 (s), 1265 (m), 1167 (m), 1137 (m), 1091 (s), 1071 (m), 1029 (w), 826 (w), 742 (w), 697 (s), 536 (m), 521 (m), 496 (m). ^{1}H NMR ($CDCl_3$, ppm) 8.0 (H_6, d, 1H), 6.8 (H3, d, 1H), 6.5 (H4, t, 1H), 7.2–6.9 (m, 15H, PPh_3); ^{13}C NMR ($CDCl_3$, ppm) 180.0 (C_2), 127.7 (C_3), 136.2 (C_4): 129.5 (C_5), l45.7 (C_6), 128.5 (C_α), 133.8 (C_β), 127.1 (C_γ): l27.0 (C_δ). FAB (*m*/*z*): 1076 (M^+), 852 (M–5-CF_3-pySe), 814 (M–PPh_3) and 589 (M–{5-CF_3-pySe}–PPh_3).

2.2.10. *[Os(pyS)$_2$(PPh$_3$)$_2$] (**10**)

Et_3N (0.04 ml, 0.276 mmol) was added to a methanolic solution of pySH (0.0293 g, 0.264 mmol). The resulting solution was stirred for 1 h and a solution of $[OsBr_2(PPh_3)_3]$ (0.15 g, 0.132 mmol) in dichloromethane was added. The reaction mixture was stirred for 2 h and the resulting solid was filtered off, washed with diethyl ether and dried under vacuum. *Anal*. Calc. for $C_{46}H_{38}N_2P_2S_2Os$ (mol. wt. 934.9): C, 59.0; H, 4.1; N, 3.0. Found: C, 58.8; H, 4.1; N, 2.7%. IR (KBr): 3437 (vb), 3054 (m), 1580 (m), 1480 (m), 1434 (m), 1382 (w), 1315 (w), 1261 (w), 1184 (w), 1144 (m), 1087 (m), 1028 (w), 801 (w), 743 (m), 697 (s), 521 (s). ^{1}H NMR ($CDCl_3$, ppm); 7.7 (H_6, d, 1H), 6.8 (H_3, d, 1H), 6.2 (H_4, t, 1H), 6.0 (H_5, t, 1H); 7.2–6.9 (m, 15H, PPh_3). FAB (*m*/*z*): 937 (M^+), 826 (M–pyS), 675 (M–PPh_3) and 562 (M–{pyS}–PPh_3).

2.2.11. *[Os(3-CF$_3$-pyS)$_2$(PPh$_3$)$_2$]·(CH$_2$Cl$_2$) (**11**)

3-CF_3-pySH (0.0472 g, 0.264 mmol), Et_3N (0.04 ml, 0.276 mmol) and $[OsBr_2(PPh_3)_3]$ (0.15 g, 0.132 mmol). *Anal*. Calc. for $C_{49}H_{38}Cl_2F_6N_2P_2S_2Os$ (mol. wt. 1155.2): C, 50.9; H, 3.3; N, 2.4. Found: C, 51.2; H, 3.0; N, 2.2%. IR (KBr): 3439 (vb), 3055 (m), 1578 (w), 1480 (m), 1433 (m), 1403 (m), 1320 (s), 1261 (w), 1201 (w), 1167 (m), 1123 (m), 1087 (m), 1047 (m), 1003 (w), 793 (w), 744 (m), 697 (s), 521 (s), 432 (w). ^{1}H NMR ($CDCl_3$, ppm) 7.8 (H_6, d, 1H), 6.2 (H_5, t, 1H); 7.2–6.9 (m, 16H, H_4, PPh_3). FAB (*m*/*z*): 1072 (M^+), 893 (M–{3-CF_3-pyS}), 810 (M–PPh_3) and 632 (M–{3-CF_3-pyS}–PPh_3). Crystals of $[Os(3\text{-}CF_3\text{-}pyS)_2(PPh_3)_2]\cdot(CHCl_3)$ suitable for X-ray studies were obtained by crystallisation of the initial product from methanol/chloroform.

2.2.12. *[Os(5-CF$_3$-pyS)$_2$(PPh$_3$)$_2$] (**12**)

5-CF_3-pySH (0.0472 g, 0.264 mmol), Et_3N (0.04 ml, 0.276 mmol) and $[OsBr_2(PPh_3)_3]$ (0.15 g, 0.132 mmol). *Anal*. Calc. for $C_{48}H_{36}F_6N_2P_2S_2Os$ (mol. wt. 1071.1): C, 53.7; H, 3.4; N, 2.6. Found: C, 54.1; H, 3.7; N, 2.7%. IR (KBr): 3432 (vb), 3056 (m), 1593 (m), 1477 (m), 1434 (m), 1382 (w), 1322 (s), 1265 (w), 1152 (s), 1118 (m), 1079 (m), 1031 (m), 819 (w), 745 (m), 697 (s), 522 (s), 430 (w). ^{1}H NMR ($CDCl_3$, ppm) 7.7 (H_6, s, 1H), 6.6 (H_3, t, 1H), 6.3 (H_4, d, 1H); 7.2–6.9 (m, 15H, PPh_3). FAB (*m*/*z*): 1072 (M^+), 893 (M–{5-CF_3-pyS}), 810 (M–PPh_3) and 632 (M–{5-CF_3-pyS}–PPh_3).

2.2.13. *[Os(3-Me$_3$Si-pyS)$_2$(PPh$_3$)$_2$] (**13**)

3-TMS-pySH (0.0483 g, 0.264 mmol), Et_3N (0.04 ml, 0.276 mmol) and $[OsBr_2(PPh_3)_3]$ (0.15 g, 0.132 mmol). *Anal*. Calc. for $C_{52}H_{54}Si_2N_2P_2S_2Os$ (mol. wt. 1079.5): C, 57.8; H, 5.0; N, 2.6. Found: C, 57.3; H, 4.9; N, 2.7%. IR (KBr): 3436 (vb), 3052 (m), 2954 (w), 1557 (w), 1480 (m), 1433 (m), 1364 (s), 1311 (w), 1247 (m), 1215 (m), 1184 (w), 1158 (m), 1134 (m), 1087 (m), 1033 (w), 845 (s), 749 (m), 697 (s), 619 (w), 522 (s), 427 (w). ^{1}H NMR ($CDCl_3$, ppm) 7.4 (H_6, d, 1H), 7.1 (H_4, d, 1H), 6.0 (H_5, t, 1H); 0.3 (CH_3, s, 9H); 7.3–7.2 (m, 15H, PPh_3); ^{13}C NMR ($CDCl_3$, ppm) 185.5 (C_2), 138.2 (C_3), 135.1 (C_4), 114.9 (C_5), l44.2 (C_6), 127.8 (C_α), 134.0 (C_β), 126.6 (C_γ), l26.8 (C_δ), –1.6 (CH_3). FAB (*m*/*z*): 1080 (M^+), 897 (M–{3-TMS-pyS}), 818 (M–PPh_3) and 633 (M–{3-TMS-pyS}–PPh_3). Crystals of $[Os(3\text{-}TMS\text{-}pySe)_2(PPh_3)_2]$ suitable for X-ray studies were obtained by crystallisation of the initial product from methanol/dichloromethane.

2.2.14. *[Os(4-CF$_3$-pymS)$_2$(PPh$_3$)$_2$] (**14**)

4-CF_3-pymSH (0.0475 g, 0.264 mmol), Et_3N (0.04 ml, 0.276 mmol) and $[OsBr_2(PPh_3)_3]$ (0.15 g, 0.132 mmol). *Anal*. Calc. for $C_{46}H_{34}F_6N_4P_2S_2Os$ (mol. wt. 1073.1): C, 51.4; H, 3.2; N, 5.2. Found: C, 51.2; H, 3.3; N, 5.4%. IR (KBr): 3438 (vb), 3056 (m), 1543 (w), 1480 (m), 1434 (m), 1384 (w), 1348 (m), 1331 (m), 1187 (m), 1142 (m), 1114 (m), 1088 (m), 1028 (w), 990 (w), 819 (w), 746 (m), 696 (s), 544 (m), 521 (s), 430 (w). FAB (*m*/*z*): 1072 (M^+), 894 (M–{4-CF_3-pymS}), 816 (M–PPh_3) and 633 (M–{4-CF_3-pymS}–PPh_3).

2.2.15. *[Os(4 6-CF$_3$Me-pymS)$_2$(PPh$_3$)$_2$] (**15**)

4,6-CF_3Me-pymSH (0.0512 g, 0.264 mmol), Et_3N (0.04 ml, 0.276 mmol) and $[OsBr_2(PPh_3)_3]$ (0.15 g, 0.132 mmol). *Anal*. Calc. for $C_{48}H_{38}F_6N_4P_2S_2Os$ (mol. wt. 1101.1): C, 52.3; H, 3.4; N, 5.1. Found: C, 52.6; H, 3.8; N, 5.0%. IR (KBr): 3433 (vb), 3055 (m), 2926 (m), 1631 (m), 1579 (w), 1537 (w), 1478 (m), 1434 (m), 1392 (m), 1310 (w), 1278 (m), 1232 (m), 1194 (m), 1147 (m), 1115 (m), 1086 (m), 800 (w), 746 (m), 698 (s), 520 (s), 430 (w). ^{1}H NMR ($CDCl_3$, ppm) 6.1 (H_5, s, 1H), 7.5–7.7 (m, 15H, PPh_3); 2.3 (CH_3, s, 3H). FAB (*m*/*z*): 1103 (M^+), 908 (M–{4,6-CF_3Me-pymS}), 840 (M–PPh_3) and 647 (M–{4,6-CF_3Me-pymS}–PPh_3).

2.2.16. *[Os(pySe)$_2$(PPh$_3$)$_2$] (**16**)

A methanolic solution of dipyridyl-2,2′-diselenide (0.0414 g, 0.132 mmol) was treated with $NaBH_4$ (0.011 g, 0.290 mmol). The mixture was stirred for 1 h and a solution of $[OsBr_2(PPh_3)_3]$ (0.15 g, 0.132 mmol) in dichloromethane was added. The reaction mixture

was stirred for 3 h and the resulting solid was filtered off under nitrogen, washed with diethyl ether and dried under vacuum (0.052 g, 30.4%). *Anal.* Calc. for $C_{46}H_{38}N_2P_2Se_2Os$ (mol. wt. 1028.9): C, 53.6; H, 3.7; N, 2.7. Found: C, 54.0; H, 3.7; N, 2.6%. IR (KBr): 3441 (vb), 3051 (m), 1580 (w), 1543 (w), 1480 (m), 1435 (m), 1311 (w), 1261 (w), 1187 (w), 1151 (w), 1121 (m), 1086 (m), 1026 (w), 851 (w), 745 (m), 698 (s), 521 (s), 432 (w). FAB (*m*/*z*): 1030 (M^+), 871 (M–pySe), 767 (M–PPh_3) and 609 (M–{pySe}-PPh_3).

*2.2.17. [Os(3-CF_3-pySe)$_2$(PPh_3)$_2$] · 2(CH_2Cl_2) (**17**)*

(3-CF_3-pySe)$_2$ (0.0593 g, 0.132 mmol), $NaBH_4$ (0.011 g, 0.290 mmol) and [$OsBr_2(PPh_3)_3$] (0.15 g, 0.132 mmol). *Anal.* Calc. for $C_{52}H_{40}F_6Cl_4N_2P_2Se_2Os$ (mol. wt. 1382.13): C, 46.9; H, 2.9; N, 2.0. Found: C, 46.7; H, 2.5; N, 2.7%. IR (KBr): 3432 (vb), 3056 (m), 1573 (m), 1478 (m), 1435 (m), 1404 (s), 1320 (s), 1261 (m), 1205 (m), 1165 (m), 1130 (s), 1090 (m), 1054 (m), 801 (m), 745 (m), 698 (s), 526 (m), 436 (w). ^{1}H NMR ($CDCl_3$, ppm) 7.7 (H_6, d, 1H), 6.9 (H_4, d, 1H), 5.8 (H_5, t, 1H), 7.5–7.0 (m, 15H, PPh_3). FAB (*m*/*z*): 1166 (M^+), 941 (M–{3-CF_3-pySe}), 904 (M–PPh_3) and 678 (M–{3-CF_3-pySe}–PPh_3). Crystals of [Os(3-CF_3-pySe)$_2$(PPh_3)$_2$] · 2(CH_2Cl_2) suitable for X-ray studies were obtained by crystallisation of the initial product from methanol/dichloromethane.

*2.2.18. [Os(5-CF_3-pySe)$_2$(PPh_3)$_2$] · 2(CH_2Cl_2) (**18**)*

(5-CF_3-pySe)$_2$ (0.0593 g, 0.132 mmol), $NaBH_4$ (0.011 g, 0.290 mmol) and [$OsBr_2(PPh_3)_3$] (0.15 g, 0.132 mmol). *Anal.* Calc. for $C_{52}H_{40}F_6Cl_4N_2P_2Se_2Os$ (mol. wt. 1382.12): C, 46.9; H, 2.9; N, 2.0. Found: C, 46.7; H, 2.5; N, 2.1%. IR (KBr): 3432 (vb), 3056 (m), 1594 (m), 1478 (m), 1434 (m), 1376 (w), 1323 (s), 1261 (m), 1164 (m), 1129 (s), 1088 (s), 1030 (m), 821 (w), 745 (m), 697 (s), 521 (s), 430 (w). ^{1}H NMR ($CDCl_3$, ppm) 7.7 (H_6, d, 1H), 6.90 (H_3, d, 1H), 6.50 (H_4, t, 1H), 7.5–7.0 (m, 15H, PPh_3). FAB (*m*/*z*): 1166 (M^+), 941 (M–{5-CF_3-pySe}), 904 (M–PPh_3) and 678 (M–{5-CF_3-pySe}–PPh_3). Crystals of [Os(5-CF_3-pySe)$_2$(PPh_3)$_2$] · 2(H_2O) suitable for X-ray studies were obtained by crystallisation of the initial product from methanol/dichloromethane.

2.3. X-ray crystallography studies

Intensity data for all compounds, except **2**, were collected using a Smart-CCD-1000 Bruker diffractometer (Mo Kα radiation, $\lambda = 0.71073$ Å) equipped with a graphite monochromator. Intensity data for compound **2** were collected using a MACH3 Enraf Nonius diffractmeter (Mo Kα radiation, $\lambda = 0.71073$ Å) equipped with a graphite monochromator. All crystals were measured at 293 K apart from compounds **13** and **18**, which were collected at 153 K. The ω scan technique was employed to measure intensities in all crystals. Decomposition of the crystals did not occur during data collection. The intensities of all data sets were corrected for Lorentz and polarization effects. Absorption effects in all compounds, except **2** and **4**, were corrected using the program SADABS [30]; absorption in **2** was corrected using semiempirical ψ scans; absorption effects in **4** were disregarded due to its twinned nature. The crystal structures of all compounds were solved by direct methods. Crystallographic programs used for structure solution and refinement were those in SHELX97 [31] and these were installed on a PC clone. Scattering factors were those provided with the SHELX program system. Missing atoms were located in the difference Fourier map and included in subsequent refinement cycles. The structures were refined by full-matrix least-squares refinement on F^2, using anisotropic displacement parameters for all non-hydrogen atoms. Hydrogen atoms were placed geometrically and refined using a riding model, including free rotation about C–C bonds for methyl groups, with C–H distances of 0.93–0.97 Å. For all compounds, hydrogen atoms were refined with U_{iso} constrained at 1.2 (for non-methyl groups) and 1.5 (for methyl groups) times U_{eq} of the carrier C atom. Disorder was typically handled by introducing split positions for the affected groups into the refinement of the respective occupancies.

Compound **4** was a merohedral twin, where the twin law is a twofold axis along the bisector of the *a* and *b* axes. This axis interchanges *h* and *k* and reverses *l*. The structure has heavy atoms such as ruthenium, so it should be possible to determine the absolute structure. The absolute structure Flack parameter *x* [32] refined to 0.37(6), so the structure was refined as a four-component twin so as to take racemic twinning into account. Only the ruthenium atom was refined using anisotropic thermal parameters. The crystallographic problems associated with this structure mean that geometrical parameters such as bond lengths and angles will not be discussed. Compound **4** will only be used to illustrate how the connectivity around the metal centre is the same as for the rest of all the ruthenium and osmium structures. On the other hand, the X-ray crystal structure of the osmium analog of this compound (compound **13**) was studied. Compound **13** was found to have an analogous unit cell and crystallises in the same space group, *P* –4 2(1) c, as one would expect given the similar covalent radii of ruthenium and osmium. This proves that the unit cell found for the ruthenium compound **4** is the correct one.

Pertinent details of the data collections and structure refinements are summarized in Tables 1 and 2. Selected bond distances and angles are given in Tables 4–11 and a summary of the important geometrical data for all compounds is given in Tables 12 and 13. Further details regarding the data collections, structure solutions and refinements are included in the Supporting Information. Ortep3 [33] drawings with the numbering schemes used are shown in Figs. 2–10.

Table 1
Summary of crystal data and structure refinement for ruthenium complexes

	Compound **2**	Compound **4**	Compound **5**	Compound **8**
Formula	$C_{25}H_{20}Cl_2F_3NPSRu_{0.5}$	$C_{26}H_{27}NPSSiRu_{0.5}$	$C_{46}H_{34}F_6N_4P_2S_2Ru$	$C_{25}H_{20}Cl_2F_3NPSeRu_{0.5}$
M	575.89	990.28	983.90	622.79
Crystal size (mm)	$0.28 \times 0.16 \times 0.12$	$0.250 \times 0.15 \times 0.10$	$0.20 \times 0.20 \times 0.20$	$0.35 \times 0.30 \times 0.20$
Temperature (K)	293(2)	293(2)	293(2)	293(2)
Wavelength (Å)	0.71073	0.71073	0.71073	0.17073
Crystal symmetry	monoclinic	tetragonal	triclinic	monoclinic
Space group	$C2/c$	$P\bar{4}2(1)c$	$P\bar{1}$	$C2/c$
a (Å)	19.820(6)	14.9520	13.7161(5)	19.5790(3)
b (Å)	11.426(3)	14.9520	13.8199(6)	11.4930(3)
c (Å)	22.877(4)	21.7030(9)	13.9510(6)	22.5770(4)
α (°)	90.00	90.00	101.665(1)	90.00
β (°)	106.91(2)	90.00	110.114(1)	107.270(2)
γ (°)	90.00	90.00	106.264(1)	90.00
V (Å^3)	4957(2)	4852.0(2)	2247.50(16)	4851.27(17)
Z	8	8	2	8
μ (mm^{-1})	0.741	0.562	0.575	2.172
Colleted reflections	5283	11643	15580	9038
Data/restraints/parameters	5133/0/313	11643/0/148	10721/0/604	4891/0/383
Goodness-of-fit	0.932	0.487	0.972	1.060
$R_1(F)$,[a]/$[I > 2\sigma(I)]$	0.0673	0.0412	0.0663	0.0254
$wR_2(F^2)$,[b]/$[I > 2\sigma(I)]$	0.1262	0.09011	0.1136	0.0662

[a] $R_1 = \sum[|F_o| - |F_c|]/\sum[|F_o|]$.
[b] $wR_2 = [\sum(F_o^2 - F_c^2)]/\sum(F_o^2)]^{1/2}$.

Table 2
Summary of crystal data and structure refinement for osmium complexes

	Compound **11**	Compound **13**	Compound **17**	Compound **18**	Compound **19**
Formula	$C_{49}H_{37}Cl_3F_6N_2P_2S_2Os$	$C_{26}H_{27}NPSSiOs_{0.5}$	$C_{25}H_{20}Cl_2F_3NPSeOs_{0.5}$	$C_{48}H_{36}F_6N_2P_2O_2Se_2Os$	$C_{42}H_{34}Cl_2F_3N_2P_2SOs$
M	1190.42	539.71	667.35	1196.85	978.81
Crystal size (mm)	$0.30 \times 0.15 \times 0.10$	$0.25 \times 0.20 \times 0.10$	$0.50 \times 0.20 \times 0.20$	$0.25 \times 0.20 \times 0.10$	$0.55 \times 0.26 \times 0.11$
Temperature (K)	293(2)	153(2)	293(2)	153(2)	293(2)
Wavelength (Å)	0.71073	0.71073	0.71073	0.71073	0.71073
Crystal symmetry	triclinic	tetragonal	monoclinic	monoclinic	monoclinic
Space group	$P\bar{1}$	$P\bar{4}2(1)c$	$C2/c$	$P2(1)/c$	$P2(1)/c$
a (Å)	12.3849(6)	14.967	19.7198(10)	23.781(9)	9.8016(18)
b (Å)	13.5911(7)	14.967	11.5642(6)	17.481(6)	35.142(7)
c (Å)	15.1235(7)	21.771(5)	22.9848(12)	11.234(4)	11.320(2)
α (°)	89.5760(10)	90.00	90.00	90.00	90.00
β (°)	87.8420(10)	90.00	106.7764(11)	90.273(8)	98.380(3)
γ (°)	69.9380(10)	90.00	90.00	90.00	90.00
Volume (Å^3)	2389.5(2)	4877.1(15)	5018.5(4)	4670(3)	3857.6(12)
Z	2	8	8	4	4
μ (mm^{-1})	3.051	2.852	4.328	4.422	3.630
Collected reflections	17239	25013	17529	23579	7922
Data/restraints/parameters	11618/0/586	6018/0/276	6239/0/303	8201/12/568	7922/0/478
Goodness-of-fit	1.166	0.902	1.033	0.972	1.003
$R_1(F)$,[a]/$[I > 2\sigma(I)]$	0.0389	0.0333	0.0329	0.0751	0.0565
$wR_2(F^2)$,[b]/$[I > 2\sigma(I)]$	0.0966	0.0589	0.0814	0.1831	0.1086

[a] $R_1 = \sum[|F_o| - |F_c|]/\sum[|F_o|]$.
[b] $wR_2 = [\sum(F_o^2 - F_c^2)/\sum(F_o^2)]^{1/2}$.

3. Results and discussion

3.1. Synthesis

Ruthenium and osmium complexes with heterocyclic thiones R-pySH or R-pymSH were all obtained in reasonable yields by adding a methanolic solution of the appropriate ligand and triethylamine to a stirred solution of the precursor $[MX_2(PPh)_3]$ in dichloromethane:

$$2[\text{R-pySH}] + 2Et_3N + [MX_2(PPh_3)_3] \rightarrow [M(\text{R-pyS})_2(PPh_3)_2] + PPh_3 + 2Et_3NHX$$
$$M = Ru,\ X = Cl;\ M = Os,\ X = Br$$

In each case the resulting solid was filtered off under nitrogen, washed with ether and dried under vacuum. Crystals of $[Ru(3\text{-}CF_3\text{-}pyS)_2(PPh_3)_2]\cdot 2(CH_2Cl_2)$ (**2**), $[Ru(3\text{-}Me_3Si\text{-}pyS)_2(PPh_3)_2]$ (**4**), $[Ru(4\text{-}CF_3\text{-}pymS)_2(PPh_3)_2]$ (**5**), $[Os(3\text{-}CF_3\text{-}pyS)_2(PPh_3)_2]\cdot(CHCl_3)$ (**11**), $[Os(3\text{-}Me_3Si\text{-}pyS)_2(PPh_3)_2]$ (**13**) and $[OsCl_2(4,6\text{-}MeCF_3\text{-}pymS)(PPh_3)_2]$ (**19**) suitable for X-ray studies were obtained by slow evaporation of solutions of the initial product in a mixture of methanol/dichloromethane – the exception being crystals of compound **11**, which were obtained by crystallisation from methanol/chloroform.

In the synthesis of the selenium derivatives **7**–**9** and **16**–**18**, the nucleophilic species was obtained by reduction of the corresponding diselenide with sodium borohydride in methanol [34]. The product was subsequently reacted with the metal-containing precursor $[MX_2(PPh_3)_3]$ according to the following general process:

$$[MX_2(PPh_3)_3] + 2Na(R\text{-}pySe) \rightarrow [M(R\text{-}pySe)_2(PPh_3)_2] + PPh_3 + 2NaX$$
$$M = Ru,\ X = Cl;\ M = Os,\ X = Br$$

Crystallisation of the products from methanol/dichloromethane gave crystals of $[Ru(3\text{-}CF_3\text{-}pySe)_2(PPh_3)_2]\cdot 2(CH_2Cl_2)$ (**8**), $[Os(3\text{-}CF_3\text{-}pySe)_2(PPh_3)_2]\cdot 2(CH_2Cl_2)$ (**17**) and $[Os(5\text{-}CF_3\text{-}pySe)_2(PPh_3)_2]\cdot 2(H_2O)$ (**18**) that are suitable for X-ray studies.

The complexes reported here are air-stable in the solid form and do not show any tendency to decomposition or oxidation. The ruthenium complexes are also relatively stable in solution but the osmium complex decomposes slowly. This fact makes it difficult to study solutions of these complexes by NMR spectroscopy or cyclic voltammetry. It is worth noting that the crystallisation of $[Os(4,6\text{-}MeCF_3\text{-}pymS)_2(PPh_3)_2]$ (**15**) from a mixture of dichloromethane/methanol allows the isolation of the osmiun(III) complex $[OsCl_2(4,6\text{-}MeCF_3\text{-}pymS)(PPh_3)_2]$ (**19**). This finding can be rationalized as being the result of nucleophilic attack of a coordinated ligand to CH_2Cl_2. This behavior has been found previously in the reaction between $[Ag(6\text{-}^tBuMe_2Si\text{-}pyS)]$ and CH_2Cl_2, for which the reaction products were isolated and characterized by X-ray diffraction [35].

3.2. Spectroscopy

The IR spectra of the complexes confirm the presence of the ligands coordinated to the metal. For example, the band attributable to the ν(N–H), which appears at 3200–3100 cm^{-1} in the free thione ligands, is absent and this indicates that the ligands are in the deprotonated form in the complexes. The strong ligand bands in the range 1640–1660 cm^{-1} are due to the presence of ν(C=N) and ν(C=C) in a non-aromatic system. In the complexes, however, these bands appear in the region 1590–1545 cm^{-1}, which is characteristic of stretching vibrations in an aromatic group [36]. These observations confirm that the ligand is present in the complexes in the thiolate form. The spectra of the complexes also show bands due to deformation of the aromatic ring, and these appear in the regions 1110–990 and 750–620 cm^{-1} [37]. The presence of triphenylphosphine unit is confirmed by a medium intensity band at 1000 cm^{-1}, which is due to ν(P–C). The spectra of trimethylsilyl derivatives **4** and **13** also show additional medium intensity bands at 3100–2900 cm^{-1}, which correspond to the vibrations of the methyl group, and a strong intensity band in the rang 845–850 cm^{-1}, which is characteristic of ν(Si–C).

In all cases the FAB mass spectra of the compounds show peaks due to the molecular ion. Signals corresponding to the loss of one of the heterocyclic ligands are also observed along with peaks corresponding to ions formed by the loss of one of the thione or triphenylphosphine molecules. The peak clusters have appropriate isotope distributions.

The triphenylphosphine proton signals in the ^1H NMR spectra of the compounds (see Section 2) appear at relatively low field, with chemical shifts between 7.5 and 6.9 ppm. These signals appear as three triplets that integrate to 6, 3 and 6 protons, respectively, and correspond to the three different types of proton in this ligand. The other signals in the spectra are due to protons in the thiolate or selenolate ligands. The most deshielded of these signals corresponds to the ring proton *ortho* to the nitrogen atom and this appears at 7.6 and 8.4 ppm. This signal is shifted to higher field with respect to that in the corresponding free ligands. The same trend is observed for the other proton signals for the aromatic rings in that they are shifted to slightly higher field in the complexes as compared to the ligands. The signals for these protons could be assigned in all cases, except in cases where the signal overlapped the large triphenylphosphine signal. For these signals it was necessary to study COSY spectra to obtain the chemical shifts for these protons. The aliphatic proton signals – in ligands that contain such substituents on the heterocyclic ring – appear at relatively high field.

The ^{13}C spectra of the ruthenium complexes contain, in all cases, signals corresponding to the different carbon atoms in the molecule (see Section 2). In these spectra the most deshielded signal is due to the carbon directly attached to the sulfur. This signal is shifted to slightly higher field in comparison to that in the free ligand. This change in chemical shift is due to the reduction in the order of the C–S bond that occurs in the transformation from thione to thionate [38]. At higher field several

spectra contain signals due to the methyl groups present in some of the ligands. However, the signals due to the quaternary carbons of the CF_3 groups – for those compounds that contain them – are not observed due to their low intensity. Poor solubility and a degree of instability mean that raesonable ^{13}C data could not be obtained for the osmium complexes. However, the presence of the trimethylsilyl group in $[Os(3\text{-}Me_3Si\text{-}pyS)_2(PPh_3)_2]$ increased the solubility and, in this case, the spectrum could be recorded (see Section 2).

3.3. Electrochemical behavior

The cyclic voltammetry results for the ruthenium complexes are shown in Table 3. In addition, a typical voltammogram for a ruthenium compound is shown in Fig. 1. In all cases, an anodic and a cathodic peak are observed and these have the characteristics of a quasi-reversible monoelectronic process.

In the pyridine-2-thionato complexes, replacement of hydrogen by a Me_3Si group results in a slight decrease in the oxidation potential. However, replacement of a hydrogen by a CF_3 group leads to a large increase in the oxidation potential. This phenomenon could be caused by a conventional substituent inductive effect on coordinated metal potentials. In such a case, the electron-withdrawing effect of the CF_3 group would make the oxidation between Ru(II)/Ru(III) more difficult and thereby shift $E_{1/2}$ to higher values. The same explanation may also apply to the complexes derived from pyrimidine-2-thionato and pyridine-2-selenolato ligands. Comparison of the $E_{1/2}$ values for the complexes of pyridine-2-thionato and pyrimidine-2-thionato shows that the these ligands are poorer electron donors than the corresponding 2-pyridine-2-thione ligands.

Comparison of the results for the pyridine-2-thionato complexes with those for the pyridine-2-selenolato complexes shows a lower oxidation potential for the Ru/Se system. This indicates that the HOMO (Se) is destabilized relative to that of the corresponding Ru/S system.

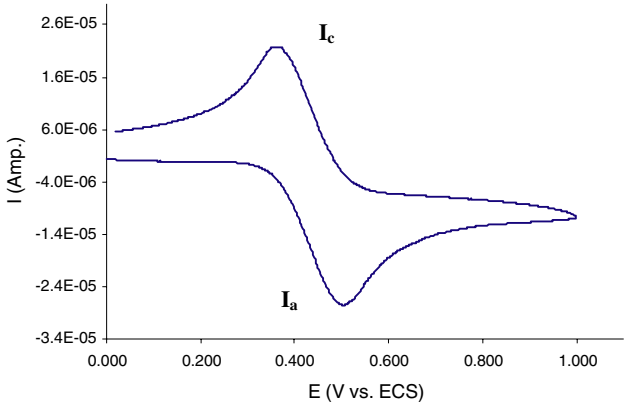

Fig. 1. Cyclic voltammogram of $[Ru(3\text{-}Me_3Si\text{-}pyS)_2(PPh_3)_2]$ in dichloromethane, scan rate 0.2 V/s.

3.4. Structural characterization

3.4.1. Molecular structures of $[Ru(3\text{-}CF_3\text{-}pyS)_2(PPh_3)_2]\cdot 2(CH_2Cl_2)$ (**2**), $[Ru(3\text{-}Me_3Si\text{-}pyS)_2(PPh_3)_2]$ (**4**), $[Ru(4\text{-}CF_3\text{-}pymS)_2(PPh_3)_2]$ (**5**) and $[Ru(3\text{-}CF_3\text{-}pySe)_2(PPh_3)_2]\cdot 2(CH_2Cl_2)$ (**8**)

The crystal structures of the ruthenium complexes are shown in Figs. 2–5 along with the numbering scheme; solvent molecules are not shown. Crystallographic data and selected distances and bond angles are given in Tables 4–6.

The presence in compound **4** of twin-type crystals (see Section 2) prevented good refinement of the structural data. This means that, although it was possible to obtain the connectivity between all the atoms in the complex, the distance and bond angle values are associated with sufficiently high level of error that they will not be included in the discussion.

The compounds are structurally very similar regardless of the nature of the thione and the substituents on the ring, which do not markedly affect the structural parameters. All of the complexes consist of neutral monomeric units with the ruthenium atom bonded to two phosphorus atoms from the triphenylphosphine

Table 3
Cyclic voltammetric data for the ruthenium complexes

L	R	$v = 0.2$ V/s				$v = 0.02$ V/s			
		E_{pc}	E_{pa}	ΔE_p	$E_{1/2}$	E_{pc}	E_{pa}	ΔE_p	$E_{1/2}$
pyS	H	0.427	0.582	0.155	0.505	0.444	0.554	0.110	0.499
	3-Me_3 Si	0.349	0.510	0.161	0.430	0.380	0.482	0.102	0.431
	3-CF_3	0.661	0.796	0.135	0.729	0.676	0.770	0.094	0.723
	5-CF_3	0.667	0.836	0.169	0.752	0.692	0.800	0.108	0.746
pymS	4-CF_3	0.851	1.028	0.177	0.940	0.880	0.988	0.108	0.934
	4,6-MeCF_3	0.783	0.908	0.125	0.846	0.792	0.886	0.094	0.839
pySe	H	0.371	0.530	0.159	0.451	0.392	0.498	0.106	0.445
	3CF_3	0.549	0.780	0.231	0.665	0.590	0.724	0.134	0.657
	5CF_3	0.603	0.766	0.163	0.685	0.628	0.724	0.096	0.676

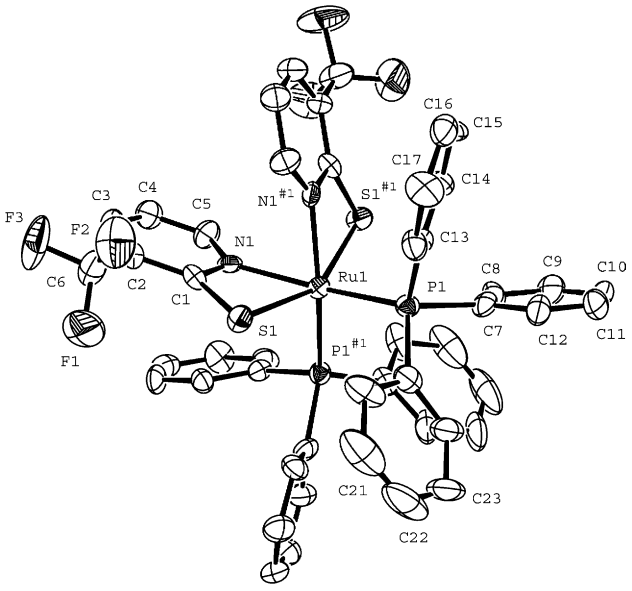

Fig. 2. Molecular structure of $[Ru(3\text{-}CF_3\text{-}pyS)_2(PPh_3)_2]\cdot 2(CH_2Cl_2)$ (**2**).

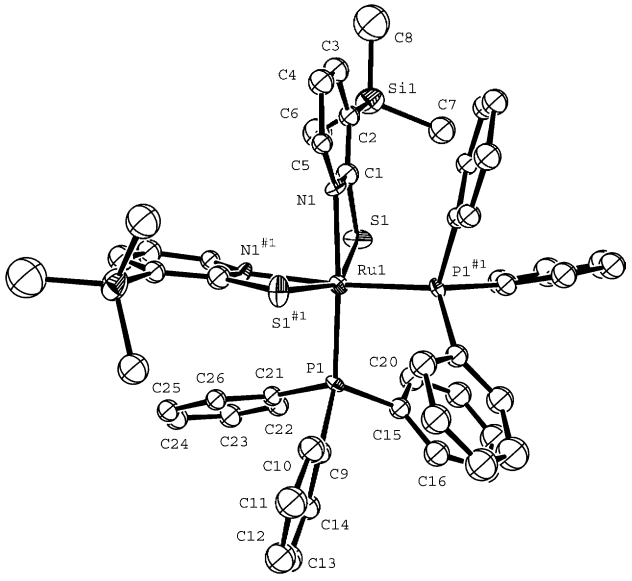

Fig. 3. Molecular structure of $[Ru(3\text{-}Me_3Si\text{-}pyS)_2(PPh_3)_2]$ (**4**).

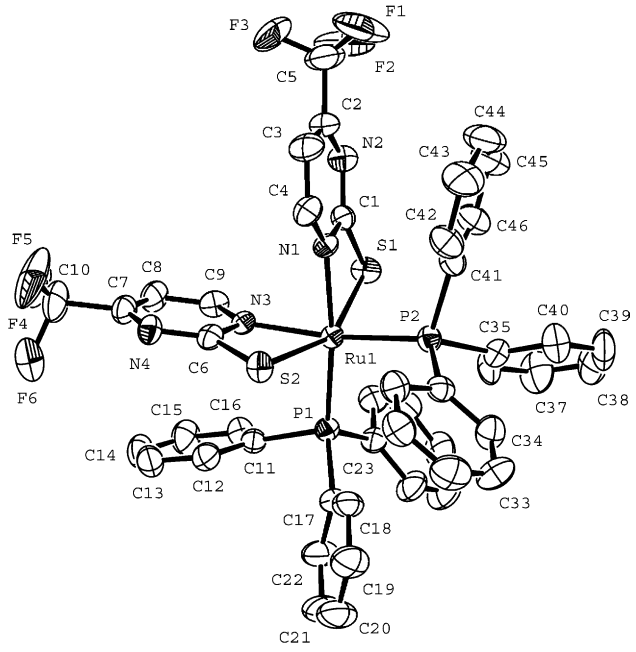

Fig. 4. Molecular structure of $[Ru(4\text{-}CF_3\text{-}pymS)_2(PPh_3)_2]$ (**5**).

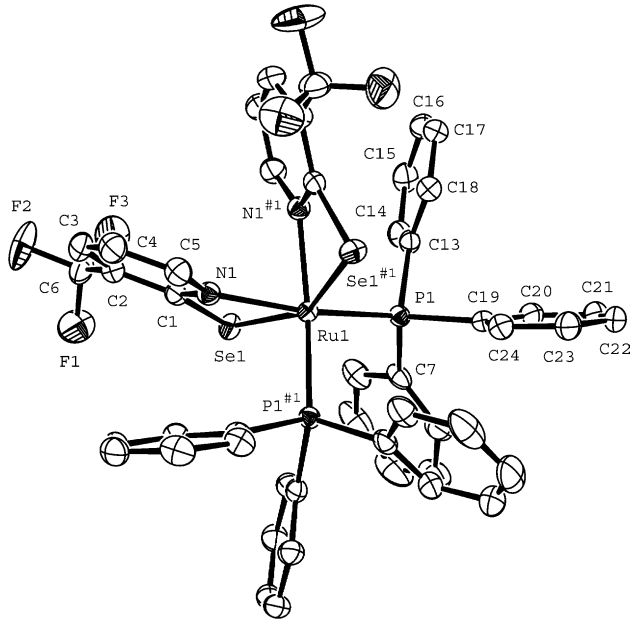

Fig. 5. Molecular structure of $[Ru(3\text{-}CF_3\text{-}pySe)_2(PPh_3)_2]\cdot 2(CH_2Cl_2)$ (**8**).

molecules, which are *cis* with respect to one another. The ruthenium is also bonded to two heterocyclic ligands that coordinate to the metal through their nitrogen and sulfur atoms – or selenium in the case of compound **8** – with these latter two atoms arranged *trans* with respect to one another.

The environment of the metal is distorted octahedral in all cases and the bond angles between the atoms arranged *trans* are markedly different from the ideal value of 180 ° (see Table 12). The main cause of this distortion is the low value for the chelate angle corresponding to the four-membered ring formed by the bidentate ligand; the values for these angles are in the range 67.21(19)–68.46(4)°.

The Ru–S bond lengths in compounds **2** and **5** are very similar and are in the range 2.416(7)–2.4327(12) Å. These values are very close to those found in other ruthenium(II) complexes with heterocyclic thione ligands (2.39–2.45 Å) [13]. The Ru–N bond lengths in all the complexes [2.086(4)–2.1467(16) Å] and the Ru–P distances [2.2936(5)–2.3566(13) Å] are also as one

Table 4
Selected bond distances (Å) and angles (°) for [Ru(3-CF_3-pyS)$_2$-(PPh_3)$_2$]·2(CH_2Cl_2) (**2**)

Ru(1)–N(1)	2.125(7)	P(1)–C(7)	1.820(9)
Ru(1)–P(1)	2.300(2)	P(1)–C(13)	1.845(8)
Ru(1)–S(1)	2.416(2)	N(1)–C(5)	1.334(9)
S(1)–C(1)	1.729(8)	N(1)–C(1)	1.376(9)
P(1)–C(19)	1.807(9)		
N(1)–Ru(1)–N(1)#1	77.1(3)	P(1)–Ru(1)–S(1)#1	98.66(8)
N(1)–Ru(1)–P(1)	163.53(18)	P(1)–Ru(1)–N(1)#1	93.67(17)
N(1)–Ru(1)–S(1)	67.21(19)	N(1)–Ru(1)–S(1)#1	90.43(19)
S(1)–Ru(1)–P(1)	99.63(8)	P(1)–Ru(1)–P(1)#1	98.28(12)

Symmetry transformation used to generate equivalent atoms: #1: $-x+1$, y, $-z+1/2$.

Table 5
Selected bond distances (Å) and angles (°) for [Ru(4-CF_3-pymS)$_2$(PPh_3)$_2$] (**5**)

Ru(1)–N(1)	2.087(3)	Ru(1)–N(3)	2.086(4)
Ru(1)–P(1)	2.3518(12)	Ru(1)–P(2)	2.3566(13)
Ru(1)–S(1)	2.4304(12)	Ru(1)–S(2)	2.4327(12)
N(1)–Ru(1)–N(3)	82.10(14)	S(1)–Ru(1)–S(2)	152.14(5)
N(1)–Ru(1)–P(1)	167.19(10)	N(3)–Ru(1)–P(1)	88.30(10)
N(1)–Ru(1)–P(2)	87.80(11)	N(3)–Ru(1)–P(2)	166.78(10)
P(1)–Ru(1)–P(2)	102.86(5)	N(1)–Ru(1)–S(1)	67.36(10)
N(3)–Ru(1)–S(1)	91.51(10)	P(1)–Ru(1)–S(1)	104.63(4)
P(2)–Ru(1)–S(1)	92.46(5)	N(1)–Ru(1)–S(2)	90.99(10)
N(3)–Ru(1)–S(2)	67.38(10)	P(1)–Ru(1)–S(2)	93.14(4)
P(2)–Ru(1)–S(2)	104.48(4)		

would expect and are similar to those found in other ruthenium(II) complexes with heterocyclic thiones and triphenylphosphine; e.g., the aforementioned complex [Ru(py)$_2$(PPh_3)$_2$], whose crystal structure has been reported (see Table 12) [8].

The structural determination of complex **8** represents the first example of a monomeric ruthenium(II) complex containing a selenolate ligand. Examples can be found in the literature of oligomeric ruthenium(II) selenolate structures in which the selenium atom acts as a bridge between metal centers. However, the only monomeric structure was reported for [Ru{Se(2,3,5,6-Me_4C_6H)}$_4$-(CH_3CN)], in which the metal is in the oxidation state IV [39] and the selenolate ligand is very hindered and acts as a terminal monodentate system. This situation means that it is impossible to make a direct comparison between the structural parameters. For example, the Ru–Se distance in **8**, 2.52456(19) Å, is markedly longer than the average value found in the Ru(IV) complex described above [2.365(3) Å]. This difference is undoubtedly due to the coordinative character of the ligand involved in each complex and the difference in the oxidation state of the metal. A better comparison is probably that with the analogous osmium complex (**17**), which is isostructural and has an analogous unit cell. The Os–Se distance in compound **17**, 2.5314(4) Å, is very similar to that in complex **8** (see below).

In these complexes the thiolate ligands are essentially planar, with S–C bond distances in the range of 1.725 at 1.733 Å (average value). These values are higher than those in the free thione [40] and this indicates that the ligands are in the thiolate form in the complexes. Other structural parameters for this ligand – as well as for the triphenylphosphine molecule – are as one would expect for this type of complex and do not warrant further attention.

Solvent molecules, in those complexes that contain them, are located within the network but do not interact significantly with the complex.

3.4.2. Molecular structures of [Os(3-CF_3-pyS)$_2$(PPh_3)$_2$]·($CHCl_3$) (**11**), [Os(3-Me_3Si-pyS)$_2$(PPh_3)$_2$] (**13**), [Os(3-CF_3-pySe)$_2$(PPh_3)$_2$]·2(CH_2Cl_2) (**17**), [Os(5-CF_3-pySe)$_2$(PPh_3)$_2$]·2(H_2O) (**18**) and [$OsCl_2$(4,6-$MeCF_3$-pymS)(PPh_3)$_2$] (**19**)

The crystal structures of the compounds under investigation are shown in Figs. 6–10 along with the numbering scheme used. Solvent molecules are not shown in these figures. Selected distances and angles for these complexes are given in Tables 7–11.

All of the complexes have similar structures and these consist of neutral monomeric units with the metal in a distorted octahedral environment. As in the case of the ruthenium complexes, the metal is coordinated by two triphenylphosphine molecules in *cis* to one another. The osmium is also coordinated by two bidentate (N, X), X = S or Se, ligands, with the X donor atoms *trans* to one another.

In a similar way to the ruthenium complexes, compounds **17** and **18** represent the first examples of

Table 6
Selected bond distances (Å) and ángles (°) for [Ru(3-CF_3-pySe)$_2$(PPh_3)$_2$]·2(CH_2Cl_2) (**8**)

Ru(1)–N(1)	2.1467(16)	Ru(1)–P(1)	2.2936(5)
Ru(1)–Se(1)	2.52456(19)	N(1)–C(5)	1.338(3)
Se(1)–C(1)	1.8834(19)	N(1)–C(1)	1.350(2)
N(1)–Ru(1)–N(1)#1A	77.03(8)	P(1)–Ru(1)–Se(1)#1	99.064(13)
N(1)–Ru(1)–P(1)#1A	93.77(4)	N(1)–Ru(1)–P(1)	163.55(4)
N(1)–Ru(1)–Se(1)	68.46(4)	N(1)–Ru(1)–Se(1)#1A	90.29(4)
Se(1)–Ru(1)–Se(1)#1	153.241(12)	Se(1)–Ru(1)–P(1)	98.368(13)
P(1)–Ru(1)–P(1)#1	98.18(3)		

Symmetry transformation used to generate equivalent atoms: #1: $-x$, y, $-z+1/2$.

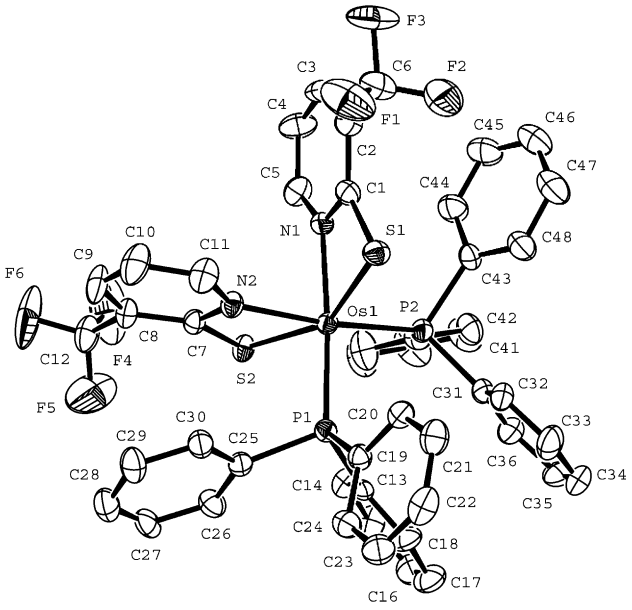

Fig. 6. Molecular structure of $[Os(3\text{-}CF_3\text{-}pyS)_2(PPh_3)_2]\cdot(CHCl_3)$ (**11**).

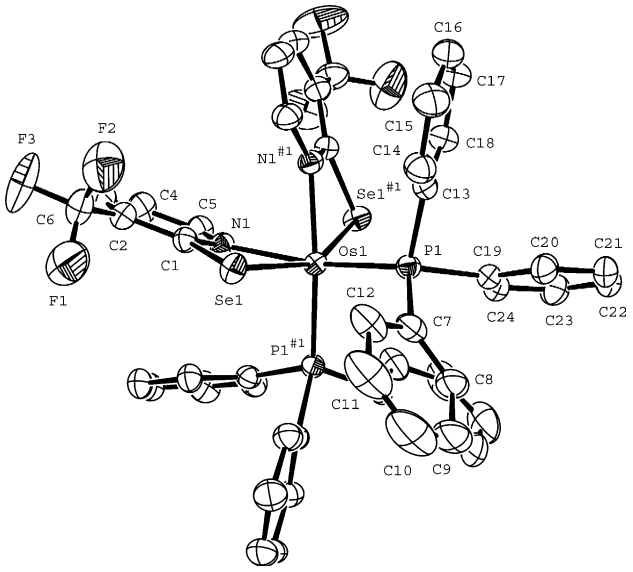

Fig. 8. Molecular structure of $[Os(3\text{-}CF_3\text{-}pySe)_2(PPh_3)_2]\cdot 2(CH_2Cl_2)$ (**17**).

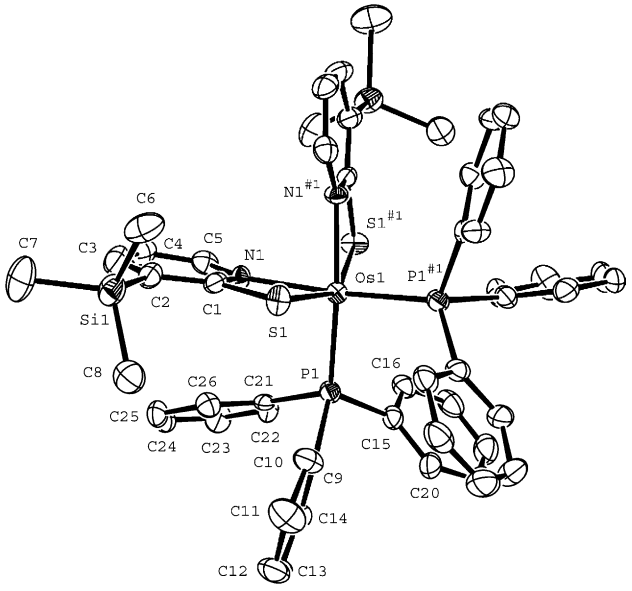

Fig. 7. Molecular structure of $[Os(3\text{-}Me_3Si\text{-}pyS)_2(PPh_3)_2]$ (**13**).

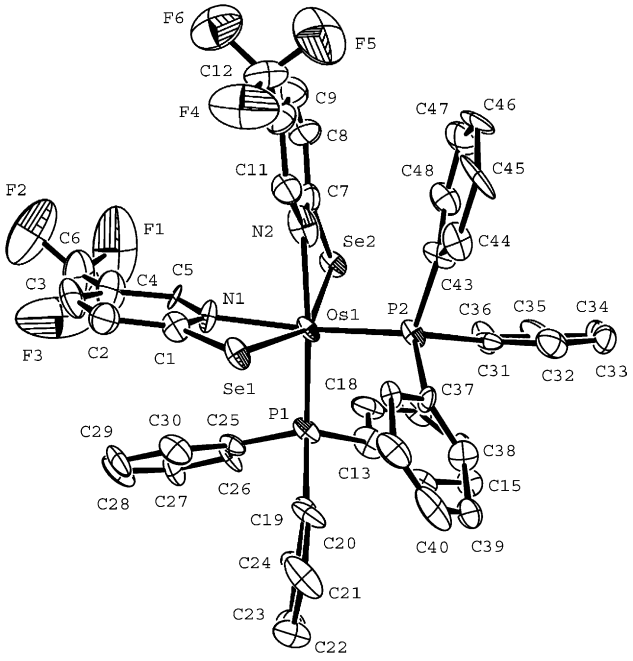

Fig. 9. Molecular structure of $[Os(5\text{-}CF_3\text{-}pySe)_2(PPh_3)_2]\cdot 2(H_2O)$ (**18**).

monomeric osmium(II) species containing selenolate ligands. A survey of the literature only reveals the crystal structures of two oligomeric osmium complexes and these contain phenylselenolate ligands. In these cases the selenium acts as a bridge between different osmium atoms [41].

The angles in the four-membered chelate rings are in the range 66.48(15)–68.12(19)°, which is again markedly different to the values one would expect for a regular geometry. In addition, the distortion in the geometry is clear from the bond angles between atoms that are *trans* to one another; these angles have values that differ significantly from the expected 180°.

The Os–S bond lengths in complexes **11** and **13**, 2.4269(15) and 2.4218(13) Å, respectively, are both similar to those found in other monomeric osmium(II) complexes with anionic heterocyclic thione N,S chelate ligands. Examples of such complexes include $[Os(\eta^2\text{-}H_2)(CO)(PPh_3)_2(pyS)](BF_4)$ [42], 2.449 Å, and $[Os(CO)_2(pyS)_2]$ [43], 2.411 and 2.419 Å. The Os–N distances in the complexes under investigation are in the range 2.102(15)–2.159(6) Å, and these values are very similar to those found in the complexes discussed above, which

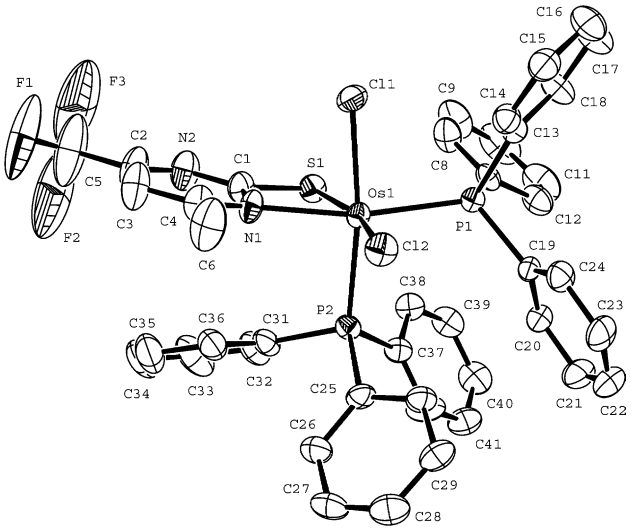

Fig. 10. Molecular structure of $[OsCl_2(4,6\text{-}MeCF_3\text{-}pymS)(PPh_3)_2]$ (**19**).

Table 7
Selected bond distances (Å) and ángles (°) for $[Os(3\text{-}CF_3\text{-}pyS)_2(PPh_3)_2](CHCl_3)$ (**11**)

Os(1)–S(1)	2.4270(15)	Os(1)–S(2)	2.4269(15)
Os(1)–N(1)	2.123(5)	Os(1)–N(2)	2.122(5)
Os(1)–P(1)	2.3126(15)	Os(1)–P(2)	2.3244(16)
S(1)–C(1)	1.742(7)	S(2)–C(7)	1.724(6)
N(1)–Os(1)–S(1)	66.48(15)	N(1)–Os(1)–S(2)	92.50(14)
N(1)–Os(1)–N(2)	81.4(2)	N(1)–Os(1)–P(1)	170.91(15)
N(1)–Os(1)–P(2)	90.31(15)	N(2)–Os(1)–S(1)	90.06(14)
N(2)–Os(1)–S(2)	66.50(14)	N(2)–Os(1)–P(1)	91.71(15)
N(2)–Os(1)–P(2)	169.01(14)	P(1)–Os(1)–P(2)	97.22(5)
P(1)–Os(1)–S(1)	107.81(5)	P(1)–Os(1)–S(2)	90.19(5)
P(2)–Os(1)–S(1)	93.26(6)	P(2)–Os(1)–S(2)	106.92(5)
S(2)–Os(1)–S(1)	151.18(5)		

Table 8
Selected bond distances (Å) and ángles (°) for $[Os(3\text{-}Me_3Si\text{-}pyS)_2(PPh_3)_2]$ (**13**)

Os(1)–N(1)	2.129(4)	Os(1)–P(1)	2.2972(13)
Os(1)–S(1)	2.4218(13)	S(1)–C(1)	1.750(5)
N(1)–C(5)	1.341(5)	N(1)–C(1)	1.361(6)
N(1)–Os(1)–N(1)#1	81.0(2)	P(1)–Os(1)–P(1)#1	95.76(6)
S(1)–Os(1)–S(1)#1	149.83(6)	N(1)–Os(1)–P(1)	93.07(11)
N(1)–Os(1)–P(1)#1	165.12(10)	N(1)–Os(1)–S(1)	66.71(10)
N(1)–Os(1)–S(1)#1	89.98(10)	P(1)–Os(1)–S(1)	100.25(5)
P(1)–Os(1)–S(1)	99.86(4)		

Symmetry transformation used to generate equivalent atoms: #1: $-x$, $-y+1$, z.

have values in the range 2.070–2.149 Å. The Os–P bond distances in the different complexes are very similar to the average value found in complexes in which the osmium is coordinated to triphenylphosphine units [44]. Finally, as mentioned previously, the absence of other structures for similar osmium selenolates makes it impossible to compare bond distances.

Table 9
Selected bond distances (Å) and ángles (°) for $[Os(3\text{-}CF_3\text{-}pySe)_2(PPh_3)_2]\cdot 2(CH_2Cl_2)$ (**17**)

Os(1)–Se(1)	2.5314(4)	Os(1)–N(1)	2.159(3)
Os(1)–P(1)	2.2962(9)	Se(1)–C(1)	1.890(4)
N(1)–Os(1)–Se(1)	67.90(8)	N(1)–Os(1)–Se(1)#1	90.25(8)
Se(1)–Os(1)–Se(1)#1	152.573(19)	N(1)–Os(1)–P(1)	162.93(9)
N(1)–Os(1)–P(1)#1	93.85(8)	P(1)–Os(1)–Se(1)	98.34(3)
P(1)–Os(1)–Se(1)#1	99.46(3)	N(1)–Os(1)–N(1)#1	76.74(16)
P(1)[a]–Os(1)–P(1)	98.54(5)		

Symmetry transformation used to generate equivalent atoms: #1: $-x$, y, $-z+1/2$.

Table 10
Selected bond distances (Å) and ángles (°) for $[Os(5\text{-}CF_3\text{-}pySe)_2(PPh_3)_2]\cdot 2(H_2O)$ (**18**)

Os(1)–Se(1)	2.5443(17)	Os(1)–Se(2)	2.5564(17)
Os(1)–N(1)	2.102(15)	Os(1)–N(2)	2.13(2)
Os(1)–P(1)	2.303(6)	Os(1)–P(2)	2.303(6)
Se(1)–C(1)	1.84(2)	Se(2)–C(7)	1.89(2)
N(1)–Os(1)–Se(1)	67.0(4)	N(1)–Os(1)–Se(2)	90.6(5)
N(1)–Os(1)–P(1)	92.2(5)	N(1)–Os(1)–P(2)	164.0(4)
N(1)–Os(1)–N(2)	81.7(6)	N(2)–Os(1)–Se(1)	90.4(4)
N(2)–Os(1)–Se(2)	68.1(4)	N(2)–Os(1)–P(1)	166.4(4)
N(2)–Os(1)–P(2)	90.6(5)	P(1)–Os(1)–Se(1)	98.36(15)
P(1)–Os(1)–Se(2)	100.05(15)	P(1)–Os(1)–P(2)	98.06(15)
P(2)–Os(1)–Se(1)	99.32(14)	P(2)–Os(1)–Se(2)	99.56(15)
Se(1)–Os(1)–Se(2)	151.39(7)		

Table 11
Selected bond distances and angles for $[OsCl_2(4,6\text{-}MeCF_3\text{-}pymS)(PPh_3)_2]$ (**19**)

Os(1)–Cl(1)	2.391(2)	Os(1)–P(1)	2.365(2)
Os(1)–Cl(2)	2.381(2)	Os(1)–P(2)	2.414(2)
Os(1)–N(1)	2.153(6)	S(1)–C(1)	1.728(9)
Os(1)–S(1)	2.363(2)		
N(1)–Os(1)–S(1)	68.12(19)	S(1)–Os(1)–P(1)	103.58(7)
N(1)–Os(1)–Cl(1)	81.8(2)	S(1)–Os(1)–P(2)	85.53(7)
N(1)–Os(1)–Cl(2)	98.71(19)	P(1)–Os(1)–Cl(1)	87.92(7)
N(1)–Os(1)–P(1)	166.8(2)	P(1)–Os(1)–Cl(2)	89.79(7)
N(1)–Os(1)–P(2)	90.5(2)	Cl(1)–Os(1)–Cl(2)	91.00(8)
S(1)–Os(1)–Cl(1)	89.43(8)	P(1)–Os(1)–P(2)	99.33(7)
S(1)–Os(1)–Cl(2)	166.63(8)	Cl(1)–Os(1)–P(2)	171.97(7)

Table 12
Summary of selected bond lengths [Å] and angles [°] for the ruthenium complexes (average values)

	(1)[a]	(2)	(5)	(8)
Ru–N	2.124(6)	2.125(7)	2.086(4)	2.1467(16)
Ru–P	2.326(2)	2.300(2)	2.3542(12)	2.2936(5)
Ru–X[b]	2.436(2)	2.416(2)	2.4315(12)	2.52456(19)
C–X	1.739(9)	1.729(8)	1.729(5)	1.8834(19)
N–Ru–X	67.1(2)	67.21(19)	67.37(10)	68.46(4)
P–Ru–N	169.0(2)	163.53(18)	166.78(10)	163.55(4)
	171.6(2)	163.53(18)	167.19(10)	163.55(4)
X–Ru–X	154.7(1)	151.88(12)	152.14(5)	153.241(12)

[a] From Ref. [8].
[b] X = S or Se.

Table 13
Summary of selected bond lengths [Å] and angles [°] for the osmium complexes (average values)

	(11)	(13)	(17)	(18)	(19)
Os–N	2.122(5)	2.129(4)	2.159(3)	2.116(15)	2.153(6)
Os–P	2.3185(15)	2.2972(13)	2.2962(9)	2.303(6)	2.389(2)
Os–X[a]	2.4269(15)	2.4218(13)	2.5314(4)	2.5503(17)	2.363(2)
C–X	1.743(7)	1.750(5)	1.890(4)	1.86(2)	1.728(9)
Os–Cl					2.386(2)
N–Os–X	66.49(15)	67.71(10)	67.90(8)	67.5(4)	68.12(19)
P–Os–N	169.01(14)	165.12(10)	162.93(9)	164.0(4)	166.8(2)
	170.91(15)	165.12(10)	162.93(9)	166.4(4)	
X–Os–X	151.18(5)	149.83(6)	152.573(19)	151.39(7)	
Cl–Os–P					171.97(7)
Cl–Os–S					166.63(8)
Cl–Os–Cl					91.00(8)

[a] (S or Se).

Complex **19** was obtained during the crystallisation of compound **15** and in this transformation one of the pyrimidine-2-thiolate molecules was replaced by two chloro ligands (vide infra). Compound **19** has a similar structure to the other osmium complexes in that the metal is in an octahedral environment and the two chloro ligands are arranged *cis* with respect to one another. Comparison of the structural data for this complex with those discussed previously shows a shorter Os–S distance, 2.363(2) Å, which is probably due to the difference in the oxidation state of the metal.

4. Conclusions

The work described in this paper involves the synthesis and structural characterization of a series of ruthenium and osmium complexes with heterocyclic bidentate (N, S) and (N, Se) donor ligands and triphenylphosphine. These ligands contain different substituents on the heterocyclic ring but it appears that the steric hindrance produced by such substituents does not significantly influence the structures of the complexes. Furthermore, the nature of the donor atoms in the heterocyclic ligand does not markedly influence the structure of the complex. All of the complexes under investigation have an octahedral structure, with the phosphorus atoms in a *cis* arrangement and the sulfur (or selenium) atoms in *trans* positions. These findings are in sharp contrast to the chemistry of other elements, for which the presence and position of substituents in the ring do have an influence on the structures of the complexes [19].

Acknowledgements

This work was supported by Xunta de Galicia (Spain) (grant PGIDT00PXI20305PR) and by the Ministerio de Ciencia y Tecnología (Spain) (grant BQU2002-01819). We are grateful to Johnson and Mathey for the loan of ruthenium and osmium salts.

Appendix A. Supplementary data

Crystallographic data for the structures reported in this paper have been deposited at the Cambridge Crystallographic Data Center as supplementary publication numbers CCDC 267446-267454. Copies of the data can be obtained free of charge on application to CCDC, 12 Union Road, Cambridge, CB2 1EZ, UK [fax: +44-1223-336-033; e-mail deposit@ccdc.cam.ac.uk]. Supplementary data associated with this article can be found, in the online version, at doi:10.1016/j.ica.2005.06.009.

References

[1] (a) A.J. Deeming, M.N. Meah, H.M. Dawes, M.B. Hursthouse, J. Organomet. Chem. 299 (1986) 25C;
(b) G. Valle, R. Ettorre, U. Vettori, V. Peruzzo, G. Plazzogna, J. Chem. Soc., Dalton Trans. (1987) 815;
(c) T.S. Lobana, P.K. Bathia, E.R.T. Tiekink, J. Chem. Soc., Dalton Trans. (1989) 749;
(d) E.C. Constable, A.C. King, C.A. Palmer, P.R. Raithby, Inorg. Chim. Acta 184 (1991) 43;
(e) K. Umakoshi, A. Ichimura, I. Kinoshita, S. Ooi, Inorg. Chem. 29 (1990) 4005.
[2] (a) E.C. Constable, P.R. Raithby, J. Chem. Soc., Dalton Trans. (1987) 2281;
(b) P. Karagiannidis, P. Aslanidis, D.P. Kessissoglou, B. Krebs, M. Dartmann, Inorg. Chim. Acta 156 (1989) 47;
(c) P. Aslanidis, S.K. Hadjikakou, P. Karagiannidis, B. Kojic-Prodic, M. Luic, Polyhedron 13 (1994) 3119.
[3] (a) P. Mura, B.G. Olby, S.D. Robinson, J. Chem. Soc., Dalton Trans. (1985) 2101;
(b) P. Mura, B.G. Olby, S.D. Robinson, Inorg. Chim. Acta 98 (1985) L21;
(c) P.D. Cookson, E.R.T. Tiekink, J. Chem. Soc., Dalton Trans. (1993) 259.

[4] (a) M.A. Ciriano, F. Viguri, J.J. Pérez-Torrente, F.J. Lahoz, L.A. Oro, A. Tiripicchio, M. Tiripicchio-Camellini, J. Chem. Soc., Dalton Trans. (1989) 25;
(b) Y. Nakatsu, Y. Nakamura, K. Matsumoto, S. Ooi, Inorg. Chim. Acta 196 (1992) 81;
(c) R. Schmiedgen, F. Huber, H. Preud, G. Ruisi, R. Barbieri, Appl. Organomet. Chem. 8 (1994) 397;
(d) M. Gupta, R.E. Cramer, K. Ho, C. Pettersen, S. Mishina, J. Belli, C.M. Jensen, Inorg. Chem. 34 (1995) 60.
[5] (a) J.H. Yamamoto, W. Yoshida, C.M. Jensen, Inorg. Chem. 30 (1991) 1353;
(b) J.G. Reynolds, S.C. Sendlinger, A.M. Murray, J.C. Huffman, G. Christou, Angew. Chem. Int. Ed. Engl. 31 (1992) 1253;
(c) H. Engelking, S. Karentzopoulos, G. Reusmann, B. Krebs, Chem. Ber. 127 (1994) 2355;
(d) R.M. Tylicki, W. Wu, P.E. Fanwick, R.A. Walton, Inorg. Chem. 34 (1995) 988.
[6] (a) N. Zhang, S.R. Wilson, P.A. Shapley, Organometallics 7 (1988) 1126;
(b) A.J. Deeming, M.N. Meah, P.A. Bates, M.B. Hursthouse, J. Chem. Soc., Dalton Trans. (1988) 235;
(c) A.J. Deeming, M.N. Meah, P.A. Bates, M.B. Hursthouse, J. Chem. Soc., Dalton Trans. (1988) 2193;
(d) M.A. Ciriano, J.J. Pérez-Torrente, F. Viguri, F.J. Lahoz, L.A. Oro, A. Tiripicchio, M. Tiripicchio-Camellini, J. Chem. Soc., Dalton Trans. (1990) 1493;
(e) O.F.Z. Khan, M. Mazid, M. Motevalli, P. O'Brien, Polyhedron 9 (1990) 541;
(f) P. Yu, L. Huang, B. Zhuang, Acta Crystallogr. C50 (1994) 1191;
(g) B.R. Cockerton, A.J. Deeming, Polyhedron 13 (1994) 2085.
[7] (a) E.S. Raper, Coord. Chem. Rev. 61 (1985) 115;
(b) I.G. Dance, Polyhedron 5 (1986) 1037;
(c) P.G. Blower, J.R. Dilworth, Coord. Chem. Rev. 76 (1987) 121;
(d) B. Krebs, G. Henkel, Angew. Chem., Int. Ed. Engl. 30 (1991) 769.
[8] S.R Fischer, A.C. Skapski, J. Chem. Soc., Dalton Trans. (1972) 635.
[9] P. Mura, B.G. Olby, S.D. Ronbinson, J. Chem. Soc., Dalton Trans. (1985) 2101.
[10] E.C. Constable, P.R. Raithby, Inorg. Chim. Acta 183 (1991) 21.
[11] A.J. Deeming, K.I. Hardcastle, M. Karim, Inorg. Chem. 32 (1992) 4792.
[12] B.K. Santra, M. Menon, C.K. Pal, G.K. Lahiri, J. Chem. Soc., Dalton Trans. (1997) 1387.
[13] B.K. Panda, S. Chattopadhyay, K. Ghosh, A. Chakraworty, Polyhedron 21 (2002) 899.
[14] T.S. Lobana, R. Verma, R. Singh, A. Castiñeiras, Transition Met. Chem. 23 (1998) 25.
[15] A. Deming, M. Meah, M. Nafees, N. Randle, K.I. Hardcastle, I. Kenneht, J. Chem. Soc., Dalton Trans. (1989) 2211.
[16] A. Demming, R. Vaish, A. Arce, Y. de Santis, Polyhedron 13 (1994) 3285.
[17] E.W. Ainscough, A.M. Brodie, R.K. Coll, K. Richard, J.M. Waters, Aust. J. Chem. 52 (1999) 801.
[18] (a) R. Castro, M.L. Durán, J.A. García-Vázquez, J. Romero, A. Sousa, A. Castiñeiras, W. Hiller, J. Strähle, Z. Naturforsch 47b (1992) 1067;
(b) R. Castro, J.A. García-Vázquez, J. Romero, A. Sousa, A. Castiñeiras, W. Hiller, J. Strähle, Inorg. Chim. Acta 211 (1993) 47.
[19] A. Sousa-Pedrares, J. Romero, J.A. García-Vázquez, M.L. Durán, M.I. Casanova, A. Sousa, J. Chem. Soc., Dalton Trans. (2003) 1379.
[20] A. Sousa-Pedrares, M.I. Casanova, J.A. García-Vázquez, M.L. Durán, J. Romero, A. Sousa, J. Silver, P.J. Titler, Eur. J. Inorg. Chem. (2003) 678.
[21] R. Dilshad, K. Hanif, M.B. Hurthouse, S.E. Kabir, K.M. Abdul Malik, E. Rosemberg, J. Organomet. Chem. 585 (1999) 100.
[22] C. Landgrafe, W.S. Sheldrick, M. Suedfeld, Eur. J. Inorg. Chem. (1998) 407.
[23] K. Yamanari, T. Nozaki, A. Fuyohiro, Y. Kushi, S. Kaizaki, J. Chem. Soc., Dalton Trans. (1996) 2851.
[24] Y. Au, K. Cheung, W. Wong, Inorg. Chim. Acta 228 (1995) 267.
[25] E. Block, G. Ofori-Okai, J. Zubieta, J. Am. Chem. Soc. 111 (1989) 2327.
[26] A.R. Katritzky, C.W. Rees, Comprehensive Heterocyclic Chemistry, vol. 3, Pergamon Press, Oxford, 1984.
[27] L. Brandsma, H.E. Wijers, Rec. Trav. Chim. Pays Bas. 82 (1963) 68.
[28] P.S. Hallman, T.A. Stephenson, G. Wilkinson, Inorg. Synth. 12 (1970) 237.
[29] P.R. Hoffman, K.G. Caulton, J. Am. Chem. Soc. 97 (1975) 4221.
[30] G.M. Sheldrick, SADABS: Program for absorption correction using area detector data, University of Göttingen, Germany, 1996.
[31] SHELX97 [Includes SHELXS97, SHELXL97, CIFTAB] – Programs for Crystal Structure Analysis (Release 97-2). G.M. Sheldrick, Institüt für Anorganische Chemie der Universität, Tammanstrasse 4, D-3400 Göttingen, Germany, 1998.
[32] H.D. Flack, Acta Crystallogr. Sect A 39 (1983) 876.
[33] ORTEP3 for Windows L.J. Farrugia, J. Appl. Crystallogr. 30 (1997) 565.
[34] S. Narayan, H. Santiesteban, J. Chem. Soc., Dalton Trans. (1998) 2359.
[35] P. Pérez-Lourido, J.A. García-Vázquez, J. Romero, M.S. Louro, A. Sousa, Q. Chen, Y. Chang, J. Zubieta, J. Chem. Soc., Dalton Trans. (1996) 2047.
[36] Spiner, J. Chem. Soc. (1960) 1237.
[37] (a) C. Paul, H.S. Makhni, P. Singh, S.L. Chadha, Z. Anorg. Allg. Chem. 337 (1970) 1332, and references therein;
(b) R.D. Kross, V.A. Fassel, M. Hargoshes, J. Am. Chem. Soc. 78 (1956) 1332.
[38] J.-M. Bret, P. Castan, G. Commenges, J.-P. Laurent, Polyhedron 2 (1983) 201.
[39] M.M. Millar, T. O'Sullivan, N. de Vries, S.A. Koch, J. Am. Chem. Soc. 107 (1985) 3714.
[40] B.R. Penfold, Acta. Cryst. 6 (1953) 38.
[41] (a) T.M. Layer, J. Lewis, A. Martín, P.R. Raithby, W.-T. Wony, J. Organomet. Chem. 444 (1993) C57;
(b) A.J. Arce, P. Arrojo, V. de Sanctis, A.J. Deeming, D.J. West, Polyhedron 11 (1992) 1013.
[42] M. Schalf, A.J. Lough, R. Morris, Organometallics 12 (1993) 3808.
[43] A.J. Deeming, M.H. Meah, N.P. Randle, K.I. Hardcastle, J. Chem. Soc., Dalton Trans. (1989) 2211.
[44] F.H. Allen, O. Kennard, R. Taylor, Acc. Chem. Res. 16 (1983) 146 (Cambridge Data Base).